



Snow thickness estimation on first-year sea ice using microwave and optical remote sensing with melt modelling

Jiacheng Zheng, Torsten Geldsetzer, John Yackel *

Cryosphere Climate Research Group, Dept. of Geography, University of Calgary, Calgary, Alberta, Canada



ARTICLE INFO

Article history:

Received 6 January 2017

Received in revised form 26 May 2017

Accepted 28 June 2017

Available online xxxx

Keywords:

Snow

Sea ice

Microwave scattering

Melt onset

Albedo

Melt ponds

Melt modelling

ABSTRACT

The snow cover on first-year sea ice plays a paramount role in thermodynamics by modulating sea ice ablation and accretion processes. However, meteoric accumulation and redistribution of snow on first-year sea ice is highly stochastic over space and time, which makes it a poorly understood parameter. In this study, a region of late-winter snow thickness on first-year sea ice in the Canadian Arctic Archipelago is estimated using time series spaceborne C-band microwave scatterometer and optical MODIS data and a simple snow melt model. Results show good correspondence between the modeled snow thickness and remotely sensed dates of melt onset and pond onset. The mean snowmelt duration for 20 study sites is 24.6 ± 1.2 days, and the estimated mean snow thickness is 14.7 ± 3.0 cm. The overall performance of the model reveals a RMSE of 4.0 cm and a mean bias of 0.3 cm. The methodology shows promise; particularly because it can easily be scaled up in order to estimate snow thickness on seasonal sea ice on a regional basis.

© 2017 Elsevier Inc. All rights reserved.

1. Introduction

One of the primary shortcomings in Global Climate Models is the inaccurate parameterization of snow covered sea ice in the polar regions. Arctic sea ice is very sensitive to temperature changes, and even small variations in temperature may trigger large effects within the climate system (IPCC, 2013). One of the most dramatic changes is the rapid reduction of multi-year sea ice (MYI) in recent years (Maslanik et al., 2007; Kwok and Rothrock, 2009). First-year sea ice (FYI), which accretes and ablates annually, continues to occupy these regions of the Arctic Ocean previously covered by MYI. These changes in MYI and FYI proportion are occurring during an overall decline of Arctic sea ice area and thickness (Lindsay and Schweiger, 2015) and are expected to impact the entire Arctic including atmospheric, oceanographic, ecological, and socio-economic systems (Post et al., 2013).

Snow cover on FYI plays a key role in sea ice thermodynamic processes (Brown and Cote, 1992; Iacozza and Barber, 2010; Webster et al., 2014; Maass et al., 2015) by modulating sea ice accretion and ablation processes. During winter, the growth of sea ice is limited due to the strong insulating properties of snow. In summer, the high albedo snow cover acts to retard sea ice melt by reflecting shortwave radiation potentially available for warming the sea ice. Due to its high albedo and

low thermal conductivity, the snow cover plays a key role in the positive feedback loop initiated by atmospheric warming (Maass et al., 2015). As a result, the warmer ocean will further contribute to sea ice thickness reductions from bottom ice melt (Eicken and Lemke, 2001) and delayed sea ice freeze-up in fall. These processes will lead to an even greater warming of the atmosphere (Moritz et al., 2002), due to enhanced evaporation and an increase to the atmospheric moisture flux, leading to a potential increase in meteoric precipitation to some regions of the marginal sea ice zone.

Meteoric accumulation and redistribution of the snow cover on FYI is highly stochastic over space and time and is generally poorly understood (Iacozza and Barber, 1999; Iacozza and Barber, 2010). An initial step towards understanding snow thickness distributions is to measure the magnitude of the snow thickness both spatially and temporally (Barber et al., 1998; Yackel et al., 2007). Previous studies show that the information about snow cover on FYI can be measured through in-situ based (e.g. Iacozza and Barber, 1999), laboratory based (e.g. Lytle et al., 1993), and remote sensing based techniques (e.g.; Barber et al., 1998; Markus et al., 2006; Yackel et al., 2007; Yackel and Barber, 2007; Kurtz et al., 2013). Owing to the logistical difficulty of direct measurement, a reliance on remote sensing techniques is required (Sturm et al., 2002; Nandan et al., 2016).

Spaceborne optical remote sensing data provide surface reflectance information (i.e. albedo) regarding snow covered FYI with a relatively fine spatial (e.g. 250 m) and temporal resolution (e.g. daily) (Hall et al., 2005). Active microwave remote sensing provides all-weather,

* Corresponding author at: Cryosphere Climate Research Group, Department of Geography, University of Calgary, 2500 University Dr NW, Calgary, AB T2N 1N4, Canada.
E-mail address: yackel@ucalgary.ca (J. Yackel).

high spatial resolution data and has demonstrated capability to characterize the seasonally evolving thermodynamic state of snow covered FYI (Livingstone et al., 1987; Barber et al., 1994).

2. Background

2.1. Seasonal evolution of snow covered FYI

The seasonal evolution of snow covered Arctic FYI is categorized into thermodynamic regimes based on the average processes operating within the system during the annual cycle (Barber et al., 1994). The categories include *freeze-up*, *winter*, *early melt*, *melt onset* and *advanced melt*. The initial freezing of Arctic seawater marks beginning of *freeze-up*, which generally occurs in October and November due to decreasing solar radiation and surface air temperature (Maykut and Untersteiner, 1971). As solar radiation and surface air temperature continue to decrease, the thin sea ice grows thicker and a layer of snow begins to accumulate on its surface. *Winter* generally occurs from December to April, and FYI typically accumulates an increasingly thicker snow cover due to cold temperatures and precipitation throughout the winter from the passage of periodic synoptic scale cyclones, which also causes significant snow redistribution (Iacozza and Barber, 2010). In late April or May, the *early melt* stage begins as snow temperature increases with increasing solar input, and the diurnal temperature range in the snow cover increases. *Melt onset* occurs in May or June when liquid water begins to accumulate near the top of the snow cover and among the interstices of the snow grains within the snow volume (Barber et al., 1994). With continued warming above 0 °C, snow water volume increases to the point where the gravity bonds break and the water drains freely to the base of the snow cover (pendular to funicular transition) (Colbeck, 1983; Barber et al., 1995). As snow continues to melt, ponds begin to appear (*pond onset*) on the FYI surface and the *advanced melt* stage begins. During this stage, a dynamic mosaic of melt ponds, bare ice and snow patches characterizes the FYI surface (Maykut and Untersteiner, 1971; Holt and Digby, 1985). As summer progresses, the ponds drain through FYI as the ice continues to melt and decay, often aided by strong winds until the sea ice breaks up and open water prevails (Hanesiak et al., 2001; Eicken et al., 2002; Eicken et al., 2004).

2.2. Backscatter and albedo interactions with seasonally evolving snow covered FYI

Active microwave interactions with snow covered FYI are a function of snow and ice electro-thermo-physical properties (Barber et al., 1998; Barber and Nghiem, 1999). The temporal evolution of the microwave backscatter coefficient (sigma nought - σ°) illustrates that a significant amount of information regarding the thermodynamic characteristics of seasonally evolving snow-covered FYI can be deduced (Barber et al., 1994; Barber et al., 1995; Grenfell et al., 1998). During *winter* and *early melt*, σ° from FYI is low and stable (Fig. 1). Smoother FYI produces a lower σ° than rougher forms of FYI, regardless of frequency (Ulaby et al., 1984). σ° occasionally oscillates during *winter* in accordance with changes in the atmospheric heat flux which causes an increase in volume scattering from the high dielectric basal snow layer which has elevated brine volume (Livingstone and Drinkwater, 1991; Barber et al., 1995; Barber and Thomas, 1998; Barber and Nghiem, 1999; Yackel and Barber, 2007). The combination of the ice surface micro- and macroscale roughness, snow grain size and brine volume (as a function of temperature and salinity) determines the overall magnitude of scattering (Barber and Nghiem, 1999).

Early melt begins when the snow volume temperature approaches -5 °C causing a rapid increase in brine volume in the basal snow layer during the warmer portion of the diurnal cycle. This causes an increase in the dielectric constant, which contributes to an increase in volume scattering (Drinkwater and Crocker, 1988; Barber et al., 1994; Golden et al., 1998). A large diurnal range in backscatter is characteristic

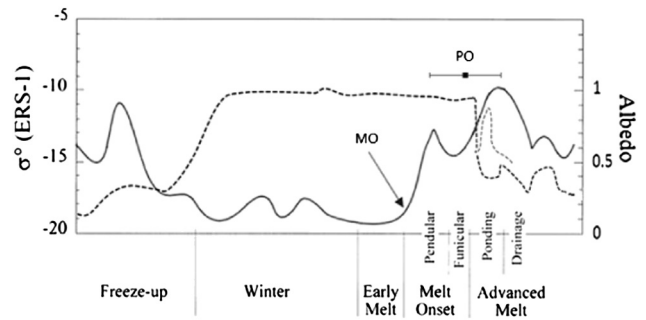


Fig. 1. Phenomenological seasonal evolution of the microwave backscatter coefficient (σ°) from C-band SAR and satellite-estimated albedo from MODIS for snow covered FYI over the seasonal periods spanning the annual cycle. The solid curve represents backscatter, and the dashed curve represents albedo. Generally, MO (melt onset) occurs at the same time for snow cover with different snow thickness; on the other hand, PO (pond onset) varies depending on snow thickness. The theoretically error bar of PO on the figure marks the timing of PO for thin and thick snow cover. The light grey dashed line depicts the albedo change for shallow pond drainage, or overnight pond refreezing, and/or snow on frozen pond during PO. (Adapted from Livingstone et al., 1987; Barber et al., 1995; Yackel et al., 2007.)

of this period owing to the increasing diurnal range in air and snow volume temperatures (Yackel and Barber, 2007).

Melt onset is denoted by a sharp increase in σ° (Fig. 1), due to increasing surface and volume scattering resulting from a continued increase in liquid water content (Livingstone and Drinkwater, 1991; Barber et al., 1995). When snow cover thickness on FYI is sufficient (typically >30 cm), there is a distinct dip in σ° corresponding with the transition from the pendular to funicular snow regimes (Colbeck, 1982; Barber et al., 1995; Yackel et al., 2007). This gravity related process marks a reduction of liquid water in the top snow layers coincident with an increase in liquid water at the base of the snow cover (Barber et al., 1995). This liquid water drainage within the snow cover during the funicular regime leads to reductions in both snow surface and volume scattering. The pendular regime appears absent when snow thickness is ≤ 10 cm (Yackel et al., 2007).

During *advanced melt*, σ° remains high over the ponding period as the overall liquid water content on the surface remains high. Melt pond surface scattering increases when wind roughened (Barber and Yackel, 1999; Yackel and Barber, 2000; Scharien et al., 2014). σ° decreases when the ponds drain through the ice leaving a lower dielectric snow and ice patch mosaic.

Similar to microwave backscatter, the presence of liquid water within the snow cover dominates the optical reflectance and albedo of FYI (Barber and LeDrew, 1994). Snow albedo is largely dependent on grain size, and decreases at all wavelengths as the grain size increases, because larger grains are both more absorptive and forward scattering than smaller grains (Wiscombe and Warren, 1980). When liquid water in the snow cover increases, it replaces air between the ice grains (Colbeck et al., 1975; Colbeck, 1979). Since the spectral refractive index of liquid water is very close to that of ice ($\sim 5 \mu\text{m}$), this replacement of air by water between ice grains can increase the effective grain size (Irvine and Pollack, 1968). Therefore, spectral albedo exhibits a general decrease for all wavelengths as liquid water content increases, which continues as the melt season progresses (Grenfell and Perovich, 2004).

The albedo of cold, dry snow on FYI during winter is high and stable (Fig. 1). Once the snow cover is >3 cm, the albedo of FYI can be as high as 0.95, especially for the case of freshly fallen meteoric snow (Brandt et al., 2005). When the snow temperature approaches 0 °C, ice grains/crystals transition to liquid water which initiates a rapid decrease the albedo, signifying *melt onset* (Perovich and Polashenski, 2012) (Fig. 1). A rapid and significant decrease in surface albedo occurs at the beginning of *advanced melt* as melt ponds begin to form on the surface. The albedo may increase temporarily if the ponds freeze over and provide a temporary platform for snow accumulation. Albedo thereafter fluctuates until sea

Download English Version:

<https://daneshyari.com/en/article/5754851>

Download Persian Version:

<https://daneshyari.com/article/5754851>

[Daneshyari.com](https://daneshyari.com)